Available online at www.sciencedirect.com
SCIENCE DIRECT®
Sedimentary Geology 187 (2006) 139–158
Sedimentary Geology
www.elsevier.com/locate/sedgeo

Inflow and outflow facies from the 1993 tsunami in southwest Hokkaido

Futoshi Nanayama [a,*], Kiyoyuki Shigeno [b]

[a] Geological Survey of Japan, AIST, Site 7, Higashi 1-1-1, Tsukuba, Ibaraki, 305-8567, Japan
[b] Meiji Consultant Co., Ltd., Chuo-ku, Sapporo 064-080, Japan Consultant Co., Ltd., S7, W1-3, Chuou-ku, Sapporo, 064-0807, Japan

Received 26 October 2004; received in revised form 7 December 2005; accepted 13 December 2005

Abstract

We describe in detail the sedimentary facies, provenance and grain-size distributions of the 1993 tsunami deposits in the lower reaches of Usubetsu River. Only two lithofacies were recognized, a gravel lobe facies (GLF) and a sand-sheet facies (SSF). The gravel lobe facies was deposited rapidly by a hydraulic jump. In contrast, the sand-sheet facies, which contains both current ripples and dunes, was deposited by a traction current under subcritical flow conditions. We identified four stratigraphic units: Unit 1, Unit 2, Unit 3, and Unit 4, in ascending order. We interpreted Units 1 and 2 as having been deposited by the inflow and outflow events of the first run-up and Units 3 and 4 by the inflow and outflow events of the second run-up, respectively. Units 3 and 4 were more widely distributed and coarser grained than Units 1 and 2 because the second run-up was larger than the first run-up. Furthermore, Unit 4 was more widely distributed than Unit 3 because the outflow eroded the inflow deposits. Grain-size distributions of the inflow and outflow deposits were clearly different. Unit 4 deposits had a peak at 2.5 phi (P-1 population). In contrast, Unit 3 deposits had a bimodal distribution with peaks at −0.5–1.5 phi (P-2 population) and at 2.5 phi (P-1 population). A comparison of the tsunami deposits with other sedimentary deposits near the study area showed that the tsunami deposits were mainly derived from the seabed at depths below 5.5 m in the offshore area, where the marine sands are about 2–2.5 phi in size and thus are the source of the P-1 population. The P-2 population is derived from coarse (0.5–2 phi) fluvial materials eroded during the tsunami run-up. According to our calculations, benthic foraminiferal tests were entrained from the comparatively deep seabed (at depths up to 100 m) during the tsunami run-up and included in the tsunami deposits.

Keywords: Tsunami deposit; Sedimentary processes; Sedimentary facies; Grain size; Benthic foraminiferal tests; 1993 Hokkaido–Nansei-oki tsunami

1. Introduction

Following the 1960 Chile tsunami, many studies on modern and ancient onshore tsunami deposits have been undertaken worldwide. For example, research carried out in Cascadia along the Pacific coast of North America (Atwater, 1987, 1992; Atwater and Moore, 1992; Clague and Bobrowsky, 1994; Benson et al., 1997; Hutchinson et al., 1997; Clague et al., 1999), Hawaii (Moore and Moore, 1984; Moore, 2000), Chile (Wright and Mella, 1963), Papua New Guinea (Gelfenbaum and Jaffe, 2003), Indonesia (Shi et al., 1995; Dawson et al., 1996; Minoura et al., 1997), northern Japan (Kon'no, 1961; Minoura and Nakaya, 1991; Minoura et al., 1994; Sato et al., 1995; Nishimura and Miyaji, 1995; Nanayama et al., 2000, 2003), Kamchatka (Minoura et

* Corresponding author. Tel.: +81 29 854 3640; fax: +81 29 852 3461.
E-mail address: nanayama-f@aist.go.jp (F. Nanayama).

0037-0738/$ - see front matter © 2006 Elsevier B.V. All rights reserved.
doi:10.1016/j.sedgeo.2005.12.024

al., 1996; Pinegina and Bourgeois, 2001), the Aegean Sea area (Minoura et al., 2000), Scotland (Dawson et al., 1988, 1991), and Norway (Bondevik et al., 1997) has shown the significance of past tsunami in relation to both hazard risk and coastal change.

Only with difficulty can past tsunami be inferred from the examination of various geological features. The difficulties in such investigations lie in distinguishing sedimentological features attributable to tsunami from similar features that may result from long-term sea-level changes, storm surges, or river floods. Because of these difficulties, investigations of sedimentary processes associated with modern tsunami such as the 1983 Nihonkai-chubu (Minoura and Nakaya, 1991), the 1992 Flores (Shi et al., 1995; Minoura et al., 1997), the 1993 Hokkaido–Nansei-oki (Sato et al., 1995; Shimamoto et al., 1995; Nishimura and Miyaji, 1995; Nanayama et al., 2000), and the 1994 Java (Dawson et al., 1996) tsunami are of considerable importance. Their value depends in part on the extent to which they are supported by eyewitness observations confirming that tsunami sediment deposition had in fact taken place in particular locations.

According to Minoura and Nakaya (1991), seawater that inundates the land as a result of a tsunami is associated with distinctive sedimentation processes and sediment deposition in marshes and coastal lagoons. Past studies of the origin of such sediments have focused on the grain-size distributions of sand layers. However, the sedimentary features of deposits emplaced by modern tsunami, such as sedimentary facies, sedimentary structures, grain-size distributions, and grain compositions, have not yet been well described and thus are not well understood. Moreover, the processes of preservation of event deposits created by huge tsunami have not been described.

The earthquake tsunami in July 1993 in southwestern Hokkaido, northern Japan, gave us an opportunity to

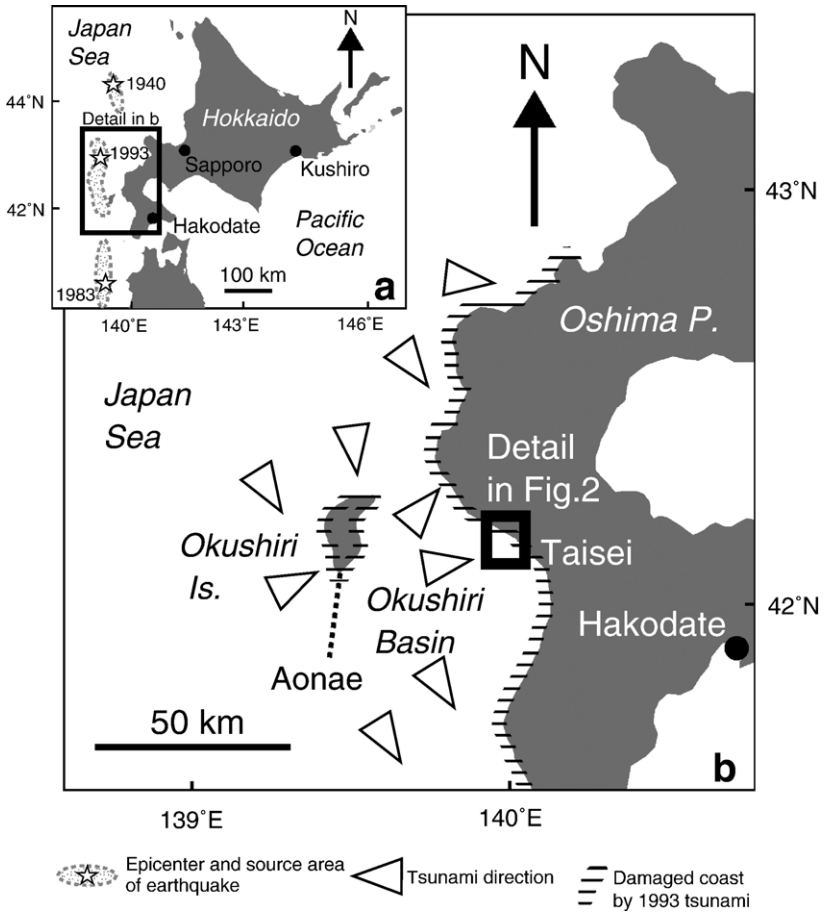

Fig. 1. (a) Map showing the location of the study area in southwestern Hokkaido. (b) The epicenter and aftershock area of the 1993 Hokkaido–Nansei-oki earthquake, and the location of the study area at Taisei along the western coast of Oshima Peninsula. White arrows show the propagation directions of the 1993 tsunami, modified after Shimamoto et al. (1995).

study in detail sediments known to have been deposited by the tsunami. We therefore carefully examined and described the 1993 tsunami deposits in the flooded area of the Usubetsu River at Taisei, along the western side of the Oshima Peninsula (Fig. 1).

2. Geomorphic setting

The Usubetsu River, which has its mouth at Taisei, is about 11 km long; its maximum width is 50 m at the Usubetsu-bashi Bridge (UB in Fig. 2). The

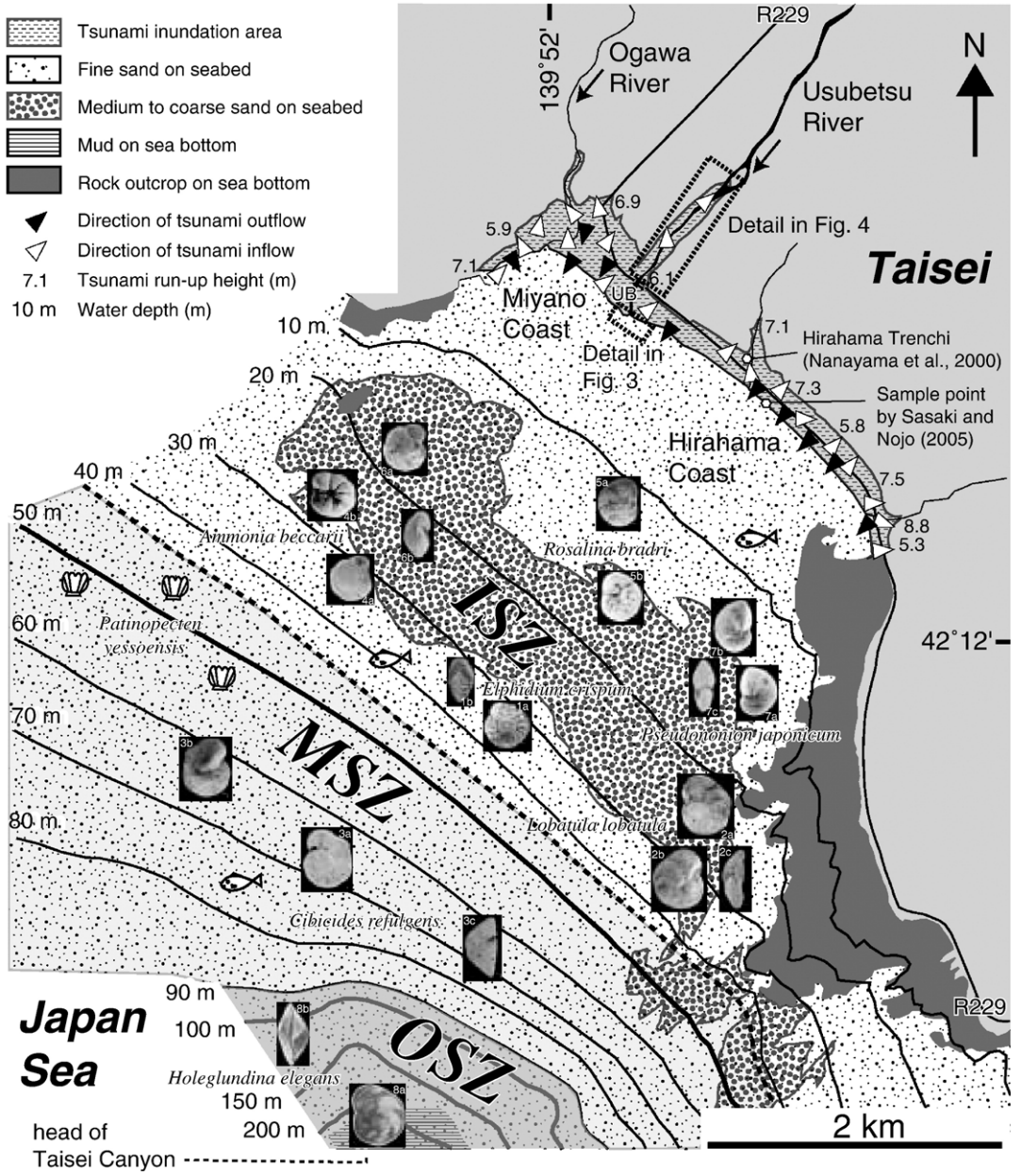

Fig. 2. Map of the onshore and offshore areas near Taisei showing the area inundated in 1993 (after Ganzawa et al., 1995) and the study area at the mouth of the Usubetsu River. Small arrows show run-inflow (white) and outflow (black) directions of the 1993 tsunami. Bathymetric distributions of modern foraminifera in the Japan Sea are shown: *E. crispum* (Linne) (1a, b); *Lobatula lobatula* (Walter and Jacob) (2a–c); *C. refulgens* Montfort (3a–c); *A. beccarii* (Linne) (4a–c and 6a, b); *Rosalina bradyi* (Cushman) (5a–c); *Pseudononion japonicum* Asano (7a–c); *H. elegans* (d'Orbigny) (8a, b). UB: Usubetsu-bashi Bridge. ISZ: inner sublittoral zone (shallower than 45 m), MSZ: middle sublittoral zone (between 45 m and 80–90 m depth) and OSZ: outer sublittoral zone (between 80–90 m depth and 190–240 m depth) defined by Akimoto and Hasegawa (1989).

river's gradient is 0.0097 in its lower reaches. It flows along the northeastern side of an alluvial plain, where its straight channel conforms to the local geological lineaments. No delta has developed at the river mouth (Fig. 2) because of strong wave action and longitudinal currents, which have formed a river-mouth bar (Fig. 3b). The river's banks are protected by concrete levees between the Usubetsu-bashi Bridge and the river mouth. The fluvial gravels and sands of the riverbed are subrounded to subangular and consist of mafic volcanic and granitic rocks (Fig. 3), derived from the geological formations in the river's upper reaches. There is a large longitudinal bar upstream of the Usubetsu-bashi Bridge (Fig. 4). This longitudinal bar also consists of fluvial gravels and is covered by modern soils and flood-plain sediments.

Along this section of coast the seafloor along this section of coast descends gradually (gradient 0.002) to a depth of 40 m about 2 km from the shore. However, at 100 m depth, the slope gradient increases suddenly to 0.02 at the head of Taisei Canyon (Fig. 2), which descends into the Okushiri basin (Fig. 1b).

The bottom sediments of Taisei between the shoreline and 200 m water depth are fine sands, and those deeper than 200 m are mud. At 20 m depth, coarse to medium sand bodies, formed by longshore currents, parallel the shoreline (Sagayama et al., 2000). The shorelines of the Miyano and Hirahama coasts are arcuate (Fig. 2). The coastal gravels are pebble- to cobble-sized, more rounded than the fluvial gravels, and of basaltic, andesitic, or granitic composition, and the coastal sands are composed of medium to coarse quartz sands derived from the Usubetsu River.

3. The 1993 Hokkaido–Nansei-oki earthquake tsunami at Taisei

At 10:17 p.m. on 12 July 1993, a magnitude 7.8 earthquake occurred with epicenter approximately 200 km northwest of Okushiri Island (42°46.8′N,

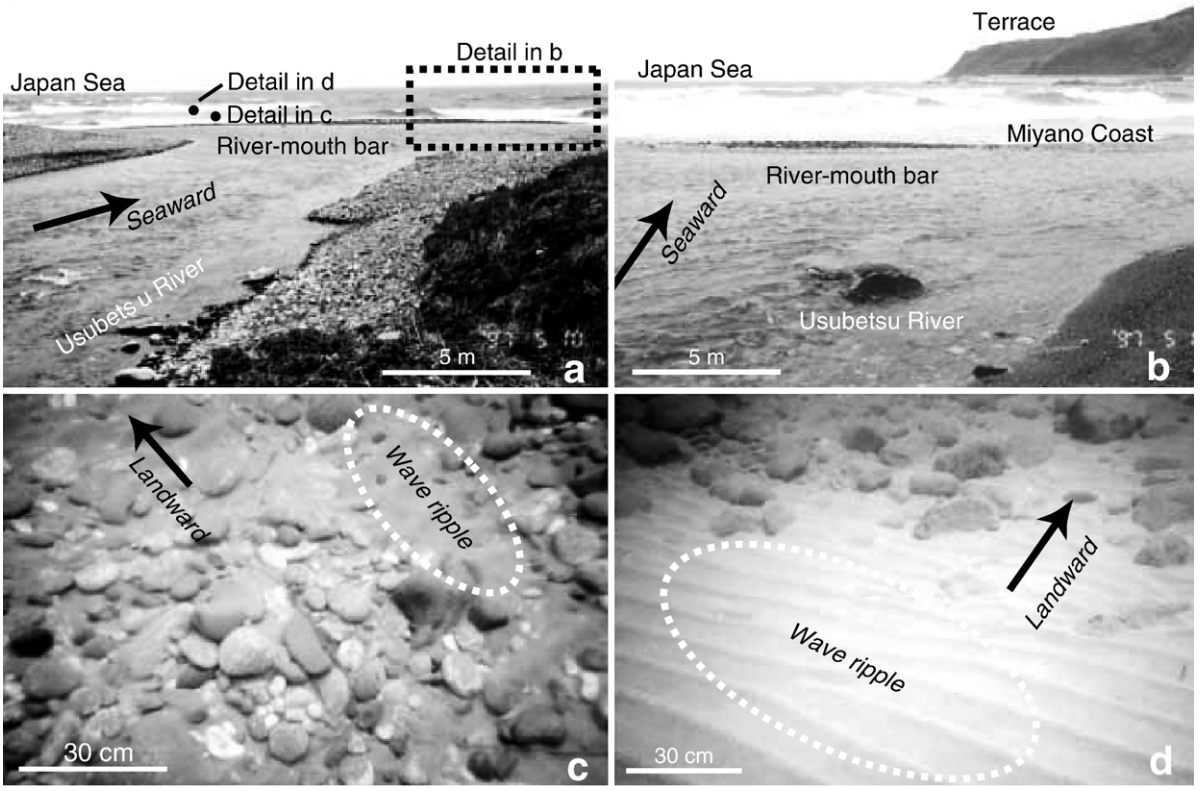

Fig. 3. Photographs showing (a) the mouth of the Usubetsu River, (b) the Miyano coast, and the seabed (c) at 0.5 m (d) and at 1 m depth off the river mouth. These photographs were taken 5 years after the 1993 tsunami. Ellipses indicate wave ripples.

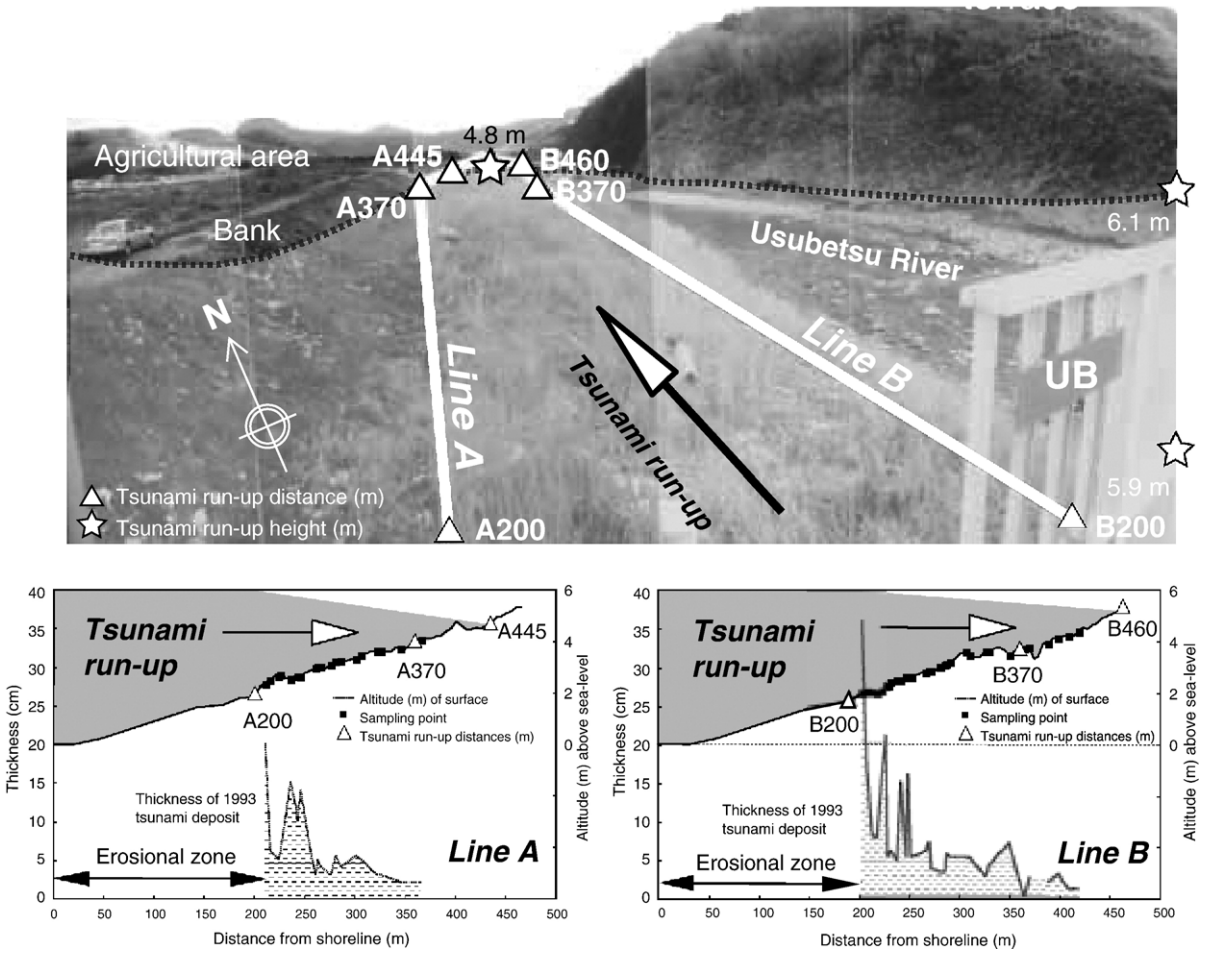

Fig. 4. An upper photograph, taken 5 years after the 1993 tsunami, looking upstream from the Usubetsu-bashi Bridge (UB in Fig. 2) along the Usubetsu River. Annotations show study area and survey lines A and B, sampling site numbers (triangles) which are also distances from the shoreline, and sites of measured heights above sea level (stars). Lower two topographic profiles, sampling site elevations and distances from the present shoreline, and thickness of the tsunami deposits along survey lines A (left) and B (right), respectively.

139°11.1′E) (Fig. 1). This Hokkaido–Nansei-oki earthquake caused a tsunami that flooded not only Okushiri Island but also parts of the western side of Oshima Peninsula in southwestern Hokkaido (Fig. 1), including Taisei town. Afterwards it was found that 230 people had been killed or were unaccounted for (Tsuji et al., 1994).

Since the tsunami arrived at night, only a few residents could provide detailed descriptions of the tsunami behavior at Taisei. According to these residents, two or three tsunami flood waves struck the Taisei area causing widespread destruction (Fig. 2). The first tsunami wave arrived at ca. 10:28 p.m., and the second wave arrived 3 min after the first, at ca. 10:31 p.m. It is not clear whether there was a third wave. If so, this wave was much smaller than the first two.

According to a post-tsunami survey, the tsunami height near Taisei was 5.3–8.8 m (Tsuji et al., 1994; Ganzawa et al., 1995; Shigeno et al., 2000). The alluvial plain at Taisei is 3 to 7 m above mean sea level, and the inundation area of the 1993 tsunami extended 300 m from the shoreline across highway R229 (Fig. 2), and 400–450 m from the shoreline along the Usubetsu and Ogawa rivers, because there were no breakwater systems at the river mouths (Fig. 2).

The tsunami ran up onto the land from the west to west–southwest (Fig. 2) at Taisei, as estimated from the collapse directions of herbaceous plants and utility poles, and from the displacement of tetrapods, observed on aerial photographs taken after the tsunami (Shigeno et al., 2000). The backwash waves converged along the Ogawa and Usubetsu rivers.

In the Usubetsu-bashi area, the first wave had a maximum height of 7.0 m, and the second wave was even higher, at 8.6 m. Observations based on aerial photographs indicated that the tsunami invasion extended 450 to 460 m inland from the shoreline at the Usubetsu River, as estimated by plant debris on the flood plain (Fig. 4). The backwash waves were channeled by the low watercourse and were also controlled by the microtopography (Shigeno et al., 2000). Nanayama et al. (2000) previously reported the results of a trench survey of the 1993 tsunami deposit on the Hirahama coast (Fig. 2).

4. Methods

During 1997–2001, we described and sampled the tsunami deposits on the longitudinal bar along the Usubetsu River from the Usubetsu-bashi Bridge to a point 260 m upstream of the bridge (Fig. 4a).

4.1. Field surveys

Two survey lines (Lines A and B) were established on the longitudinal bar at approximately right angles to the recent shoreline (Fig. 4a). Altitudes and distances from the shoreline were measured by a Total Station DTM-500 (Nikon-Trimble Co., Ltd.) at all sampling points (Fig. 4b, c). We attempted to trace the tsunami deposits by collecting scoop samples every 5 m. Fifty pits, <50 cm long × 30 cm wide × 30 cm deep, were dug, and we collected 10 in situ peel samples (50 cm high × 30 cm wide) using spray-bond adhesive. Twenty-two oriented lunchbox samples (15 cm high × 20 cm wide × 3 cm deep) were collected from selected walls of these pits. The gravel fabrics, clast sizes, and compositions of three pit walls near the bridge were recorded.

4.2. Sediment descriptions

In the laboratory at the Geological Survey of Japan, AIST, the lunchbox samples were opened and oriented peels were made using the lunchbox method (Nanayama and Shigeno, 1998). By this method, we easily and quickly obtained thick oriented peels of the unconsolidated sediments, using only a plastic lunchbox and a spray-bond adhesive. A three-dimensional analysis of the sedimentary structures of the peels was carried out in the same way as with lithified sedimentary rocks.

The sedimentary facies, sedimentary structures, grain size, and colors of each sample were described. A binocular microscope was used to determine the mineral compositions of the sand grains.

4.3. Grain-size analyses and foraminiferal assemblage analyses

After the peels were taken from the 22 lunchbox samples, the remainder of each sample was sieved through 2 mm (−1 phi) and 0.062 mm (4 phi) sieves and weighed. All tests of benthic foraminifera in 10 g of the >0.062 mm residuum of each sample were picked out and identified. The mud (<0.062 mm) content (%) was estimated as the difference between the total sample weight and the weights of the sand and gravel contents. The grain sizes of the air-dried sand fractions were determined by an automatic grain-size analyzer with a settling tube (Kumon and Tateishi, 1998). The inner diameter of the settling tube was 14 cm, and the height of the water column was 150 cm. In this paper, grain size is reported as phi values, determined as follows:

$$\text{phi } (\phi) = -\log_2 d \quad (1)$$

where d is the grain size in millimeters.

5. Results

5.1. General characteristics of the tsunami deposits

The 1993 tsunami deposits were observed in many pit walls between 200 m and 430 m from the present shoreline (Fig. 4). The deposits, which were underlain by the buried 1993 surface soil, were up to 36 cm thick and some were covered by flood deposits (B420 in Fig. 5).

At B210 (Figs. 4 and 5), the tsunami deposits reached their maximum thickness of 36 cm. They consisted mainly of cobbles and pebbles (maximum diameter, 20 cm) and pebbly coarse sands (Figs. 5 and 6). These coarse deposits were found only near the Usubetsu-bashi Bridge, and they have a clear lobe-shaped distribution.

Between B216 and B250 (Fig. 4), sheeted sand layers more than 10 cm thick were composed of a fine sand with medium to coarse sand grains and gravel. Thin, fine sand layers were found between B250 and B420. Beyond B420, the deposits were lenticular, and they pinched out at B430 (Fig. 5).

Generally, the thickness of the tsunami deposits decreases away from the shoreline, but locally their thickness reflected irregularities of the land surface (Fig. 4b, c). When the tsunami inundation area reported by Ganzawa et al. (1995) is compared with the upstream limit of the tsunami deposits in this study, the former

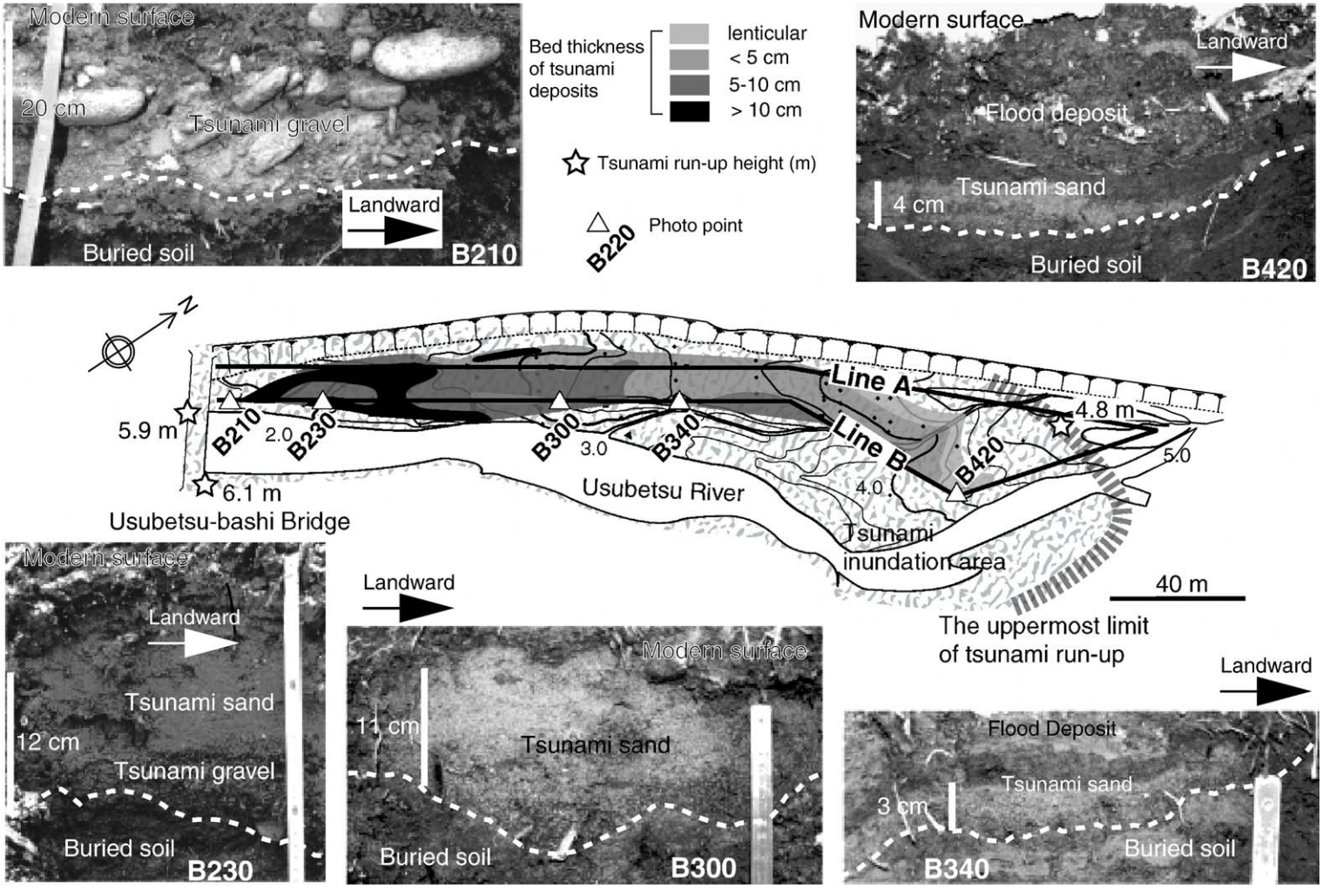

Fig. 5. Photographs showing two typical lithofacies of 1993 tsunami deposits and the locations where the five photographs were taken. The gravel lobe facies (GLF) is at the top left; the other photos show the sand-sheet facies (SSF). Photo number also gives distance from shoreline in Fig. 4.

extends 24 m further from the shoreline than the latter, but the altitudinal difference in maximum run-up is only 58 cm (Fig. 4).

5.2. Stratigraphic units and their sedimentary structures

In this study, we recognized many sedimentary structures, including gravel fabrics, current ripples, and dunes (Fig. 6). These sedimentary structures clearly show that the 1993 tsunami deposits were deposited by currents. In particular, these sedimentary structures provide information about flow directions, allowing us to distinguish inflow deposits from outflow deposits.

We have identified two sedimentary facies, a gravel lobe facies (GLF) and a sand-sheet facies (SSF), in this area. The gravel lobe facies, which has a gravel fabric, was previously described in the trench on the Hirahama Coast as having been deposited by the inflow of the second wave (Nanayama et al., 2000). On the other hand, the sand-sheet facies shows current ripples and dunes, bed forms typically produced by a traction current.

On the basis of the sedimentological characteristics, we identified four stratigraphic units from their sedimentary structures, Unit 1, Unit 2, Unit 3, and Unit 4 in ascending order. The lower boundary of each unit was clearly erosional (Figs. 6 and 7). Moreover, we identified reworked sediments above the four units at A260, B216, and B230 (Fig. 7). This reworking was caused by river flooding just after the 1993 tsunami.

5.2.1. Unit 1

Unit 1 is found only at B210 and A225, near the bridge. It overlies the 1993 soil with an erosional boundary and fills small topographic depressions (Fig. 8). The upper boundary of the unit is also erosional.

The Unit 1 deposits consist of a gravel lobe facies, comprising mainly thick-bedded, matrix-supported pebbly sands containing cobbles (maximum diameter 16 cm) with graded or inverse graded structure and a weak gravel fabric. Compositionally, the gravel assemblage is similar to that of the fluvial gravels. Gravel fabrics at A225 indicate a landward flow direction.

5.2.2. Unit 2

Unit 2 is also found only at A225 and B210 near the bridge (Fig. 7). This unit consists of a sand-sheet facies, composed mainly of fine sands with a weakly graded structure. The sediments of this unit fill small topographic depressions. Unit 2 overlies Unit 1 or the 1993 soil with an erosional boundary. No information on current direction was obtained from this unit.

5.2.3. Unit 3

Unit 3 is distributed between B210 and B250 and between A210 and A320 (Fig. 8). It overlies Unit 1 or Unit 2 or the 1993 soil with an erosional boundary and consist of two sedimentary facies, a gravel lobe facies and a sand-sheet facies.

The gravel lobe facies is distributed between B210 and B216 and consists of matrix-supported conglomerates with graded or inverse graded structure and a gravel fabric. The matrix is composed of coarse to fine sands, which contain cobbles (maximum diameter 26 cm) and fragments of shells, such as *Patinopecten yessoensis*, which inhabits the nearshore area at depths of 50–60 m off Taisei. The composition of these gravels is similar to that of the fluvial gravels. Gravel fabrics at A225 clearly show a landward current direction.

The sand-sheet facies is composed mainly of fine sands with graded structure and current ripples indicating a landward flow direction (Figs. 7 and 8). It is present at B250 and between A240 and A320. Layers of silt with wood and plant fragments are found at the top of the unit.

5.2.4. Unit 4

Unit 4 deposits are widely distributed between B210 and B430, overlying Units 1 to 3 and the 1993 soil with an erosional boundary. This unit consists only of a sand-sheet facies, composed mainly of fine sands with graded structure and current ripples indicating a seaward flow direction (Figs. 7 and 8).

5.3. Interpretation of the four stratigraphic units

We interpreted the four units in light of the two known 1993 tsunami run-up processes in the Usubetsu River and on the basis of the results reported by Nanayama et al. (2000) and eyewitness observations of the behavior of the 1993 tsunami at Taisei reported by Tsuji et al. (1994), Ganzawa et al. (1995) and Shigeno et al. (2000).

The gravel fabric of Unit 1 shows a landward flow direction. We infer that Unit 1 was deposited during the initial inflow because it is the lowest unit in the tsunami sequence. Unit 3 consists of both a gravel lobe facies and a sand-sheet facies. The fabric of the gravel lobe facies shows a landward flow direction (Figs. 7 and 8). Moreover, we identified dunes at B220, B230, and B245 and current ripples at A280 and A320 in the sand-sheet

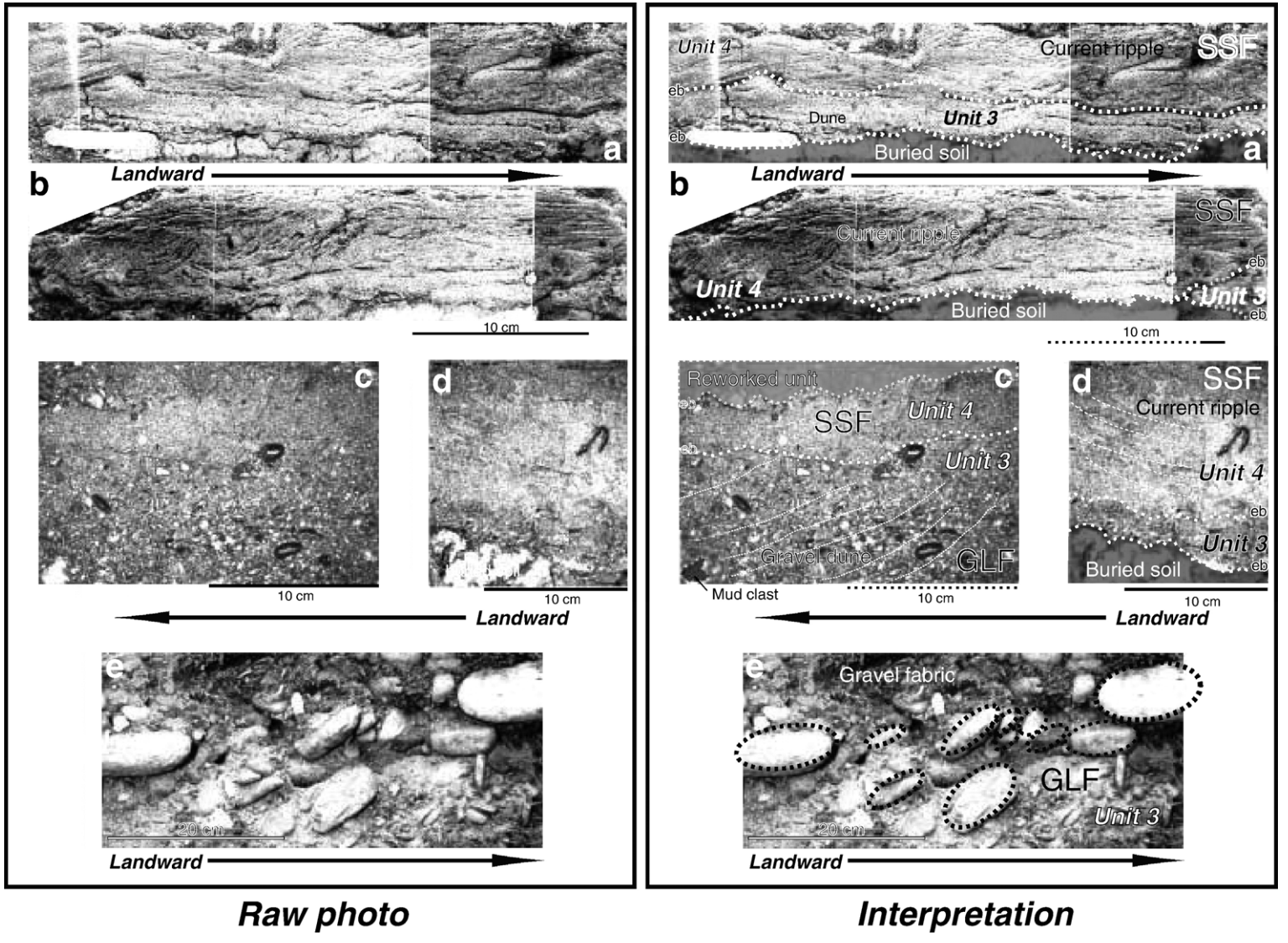

Fig. 6. Interpreted examples of sedimentary structures in the tsunami deposits, showing current ripple, dune, and gravel fabrics. The photograph of the sample is shown in the left hand, and also those interpretation charts are shown in the left hand. (a, b) Sample of the sand-sheet facies collected by the peel method at B245. (c, d) Samples of the sand-sheet facies collected by the lunch box method at B216 and A260, respectively. (e) Typical gravel fabric in the gravel lobe facies at B210. Sedimentary unit boundaries are also shown; eb: erosional boundary.

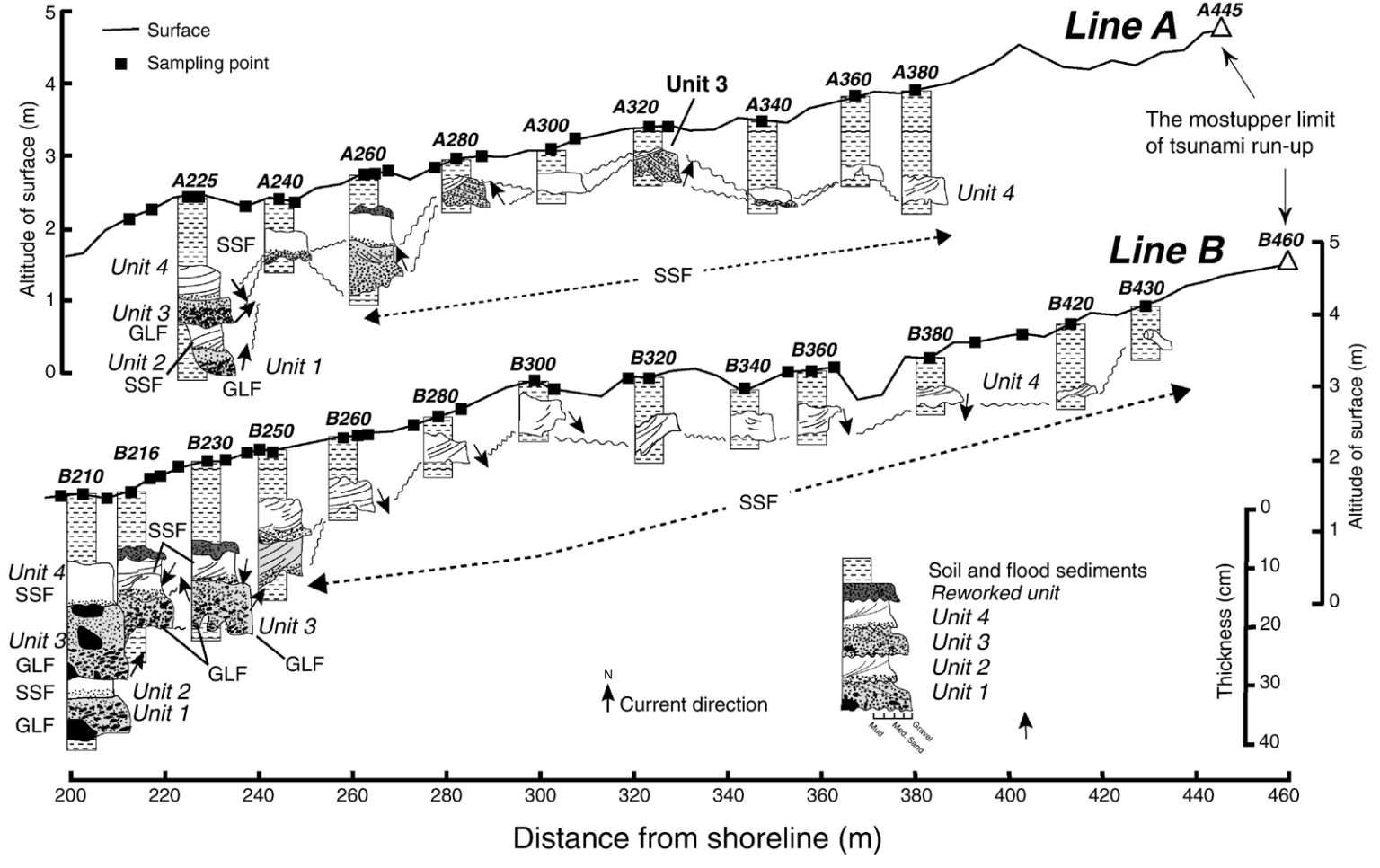

Fig. 7. Sedimentary columns along the two survey lines and correlations of the four sedimentary units between sampling locations.

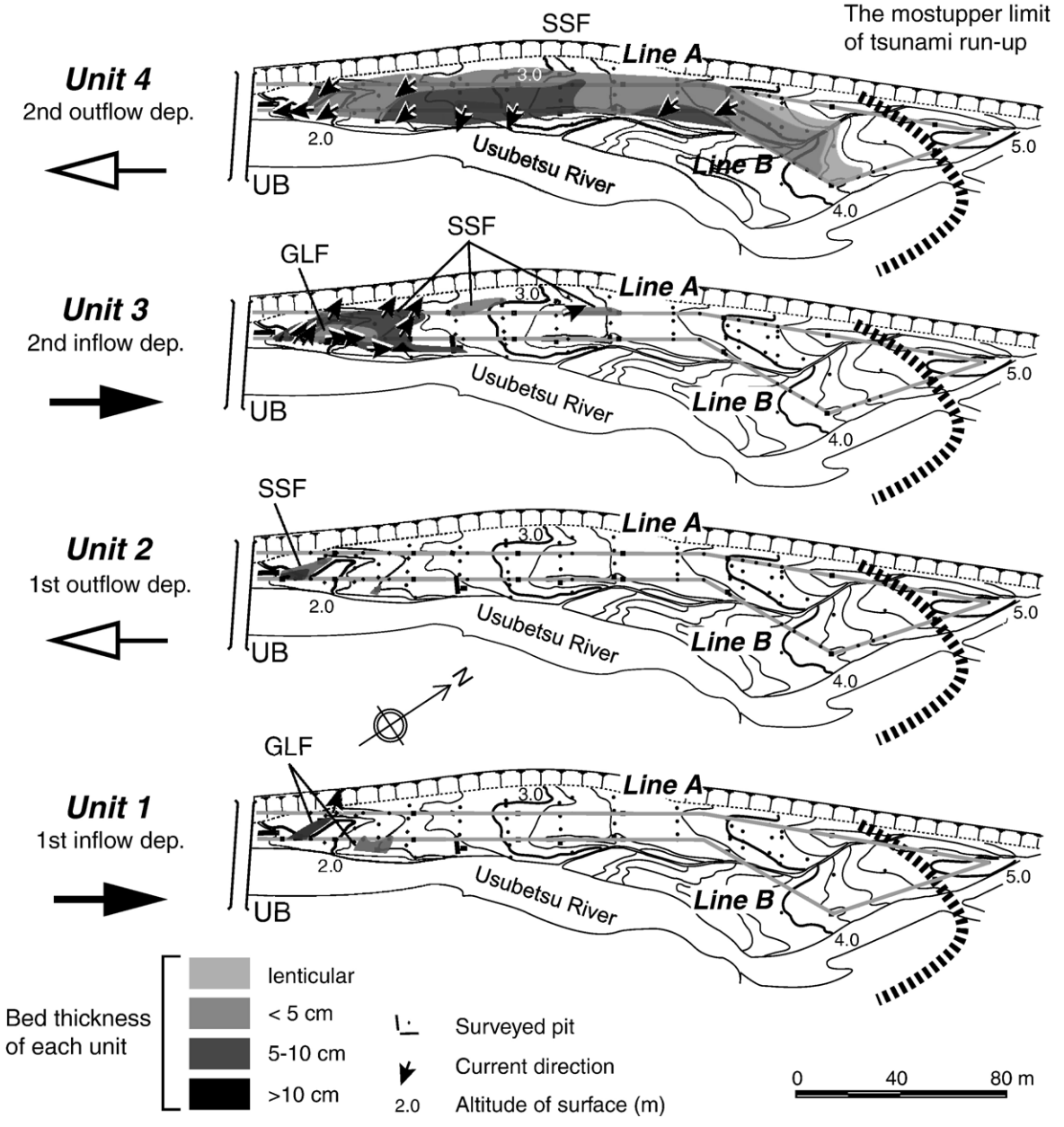

Fig. 8. Distribution maps of the four sedimentary units showing the inflow and outflow directions.

facies. From its sedimentary characteristics, we interpreted this unit as clearly deposited during inflow (Figs. 7 and 8). Furthermore, Unit 3 is capped by a thin silt layer containing many plant fragments, indicating that the silt settled while the land was flooded. On the other hand, the current ripples of Unit 4 indicate an outflow direction (Figs. 7 and 8).

These observations enabled us to interpret Unit 1 as deposits of the first inflow. There are no current data from Unit 2, but we assume on the basis of its stratigraphic position between Units 1 and 3 that Unit 2 is the first outflow deposit. Similarly, we interpret Unit 3 as having been deposited by the second inflow, and Unit 4 by the second outflow (Fig. 8).

Units 3 and 4 are more widely distributed than Units 1 and 2, and they are coarser grained, because the second run-up was larger than the first (Figs. 7 and 8). Unit 4 is more widely distributed than Unit 3 because the outflow eroded the inflow deposits of Unit 3 (Figs. 7 and 8).

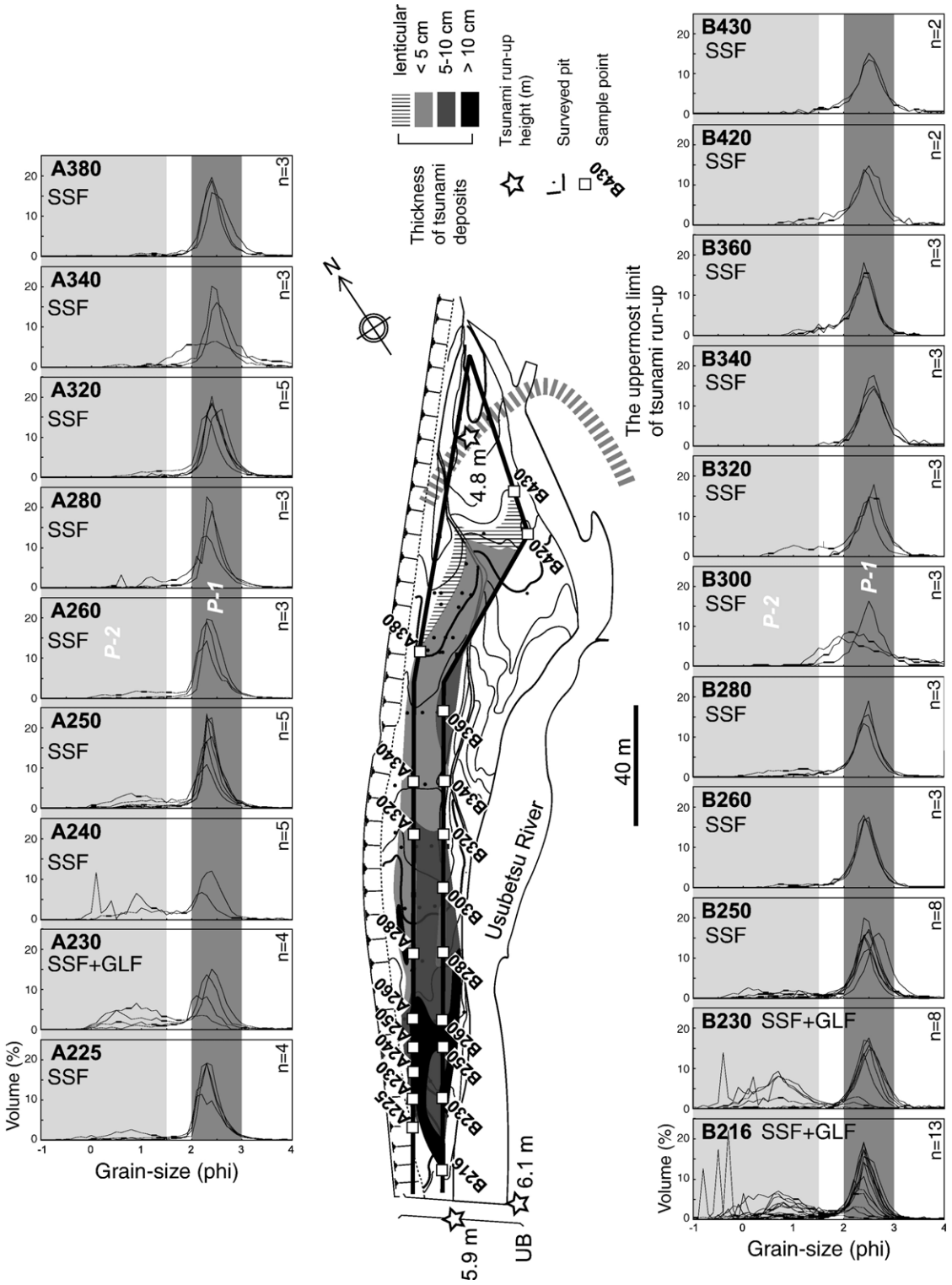

Fig. 9. Grain-size distributions of the tsunami deposits at all sampling sites along the two survey lines. P-1 and P-2 indicate two populations of grain sizes.

5.4. Grain-size distributions

In this study, we carried out a grain-size analysis of 86 samples (Fig. 9). In general, the mud content of all samples was 1–3%, and the gravel content was 0–50%. Four sites (B210, B216, B230, and A225) had a high gravel content of 30–50%. These sites were those nearest the Usubetsu-bashi Bridge.

The grain-size distributions of the inflow and outflow deposits were difficult to distinguish. The outflow deposits (Units 2 and 4) consisted of a sand-sheet facies with a peak size frequency at 2.5 phi (P-1 population). However, the grain-size distribution of the inflow deposits (Units 1 and 3), which comprised both a gravel lobe facies and a sand-sheet facies, was bimodal, with peaks at about −0.5–1.5 phi (coarse to very coarse sand, P-2 population) and 2.5 phi (fine sand, P-1 population) (Fig. 10a). Furthermore, the frequency of the P-1 population did not change with distance from the shoreline, whereas that of the P-2 population decreased with distance from the shoreline (Fig. 9). We concluded that the sand grains of the P-1 and P-2 populations had different provenances and were deposited by different sedimentary processes.

Therefore, we compared the P-1 and P-2 populations with the grain-size distributions of fluvial sands of the Usubetsu River (7 samples), beach sands of the Hirahama (11 samples) and Miyano (14 samples) coasts, and offshore sands at 5.5 m depth (4 samples; Fig. 3c, d) (Fig. 10b). Like the P-2 population, fluvial sands of the Usubetsu River have a distribution peak at 0–1.5 phi (medium to coarse sands). The grain-size distribution of the river-mouth sand was bimodal, with peaks at 1.0–2.5 phi (fine to medium sands) and 0.5–1.5 phi (medium to coarse sands), similar to the sands in the tsunami inflow deposits. However, the offshore sands had different grain-size distributions, depending on depth. At 5.5 m depth, they were fine sands, with a peak at 2–2.5 phi, similar to the P-1 population (Fig. 10). The geological map of Taisei (Sagayama et al., 2000) shows bands of fine to medium sand with a peak at 2 phi between 15 m and 35 m depth and fine sands with a peak at 2.5 phi, similar to P-1, between 35 m and 172 m depth (Fig. 2).

Therefore, we inferred that the 1993 tsunami deposits were derived mainly from fine offshore sands from depths >5.5 m depth (peak 2–2.5 phi, P-1 population) and from medium to coarse fluvial sands (peak 0.5–2 phi, P-2 population) in the study area. Thus, the P-1 tsunami sands were mainly derived up from offshore and then transported landwards by the tsunami inflows. During the tsunami run-up process, these marine sands became mixed with fluvial sands due to the turbulent flow of the run-up wave. Where the flow velocity decreased, the sands settled and were deposited.

5.5. Foraminiferal assemblages

Among the 22 lunchbox samples, we found foraminiferal tests only in samples from Unit 3 at B216 and

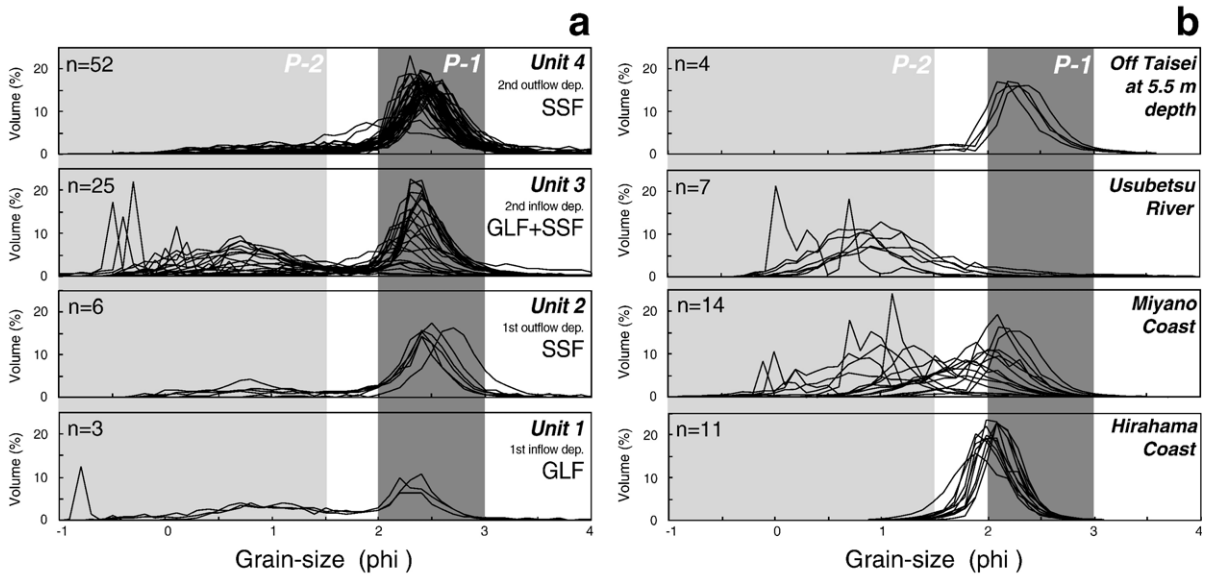

Fig. 10. Grain-size distributions arranged by (a) sedimentary unit and (b) those of fluvial, coastal, and offshore sands from below 5.5 m depth. Note the distributions of the P-1 and P-2 size modes.

Unit 4 at A300. We identified only 22 benthic species, because the foraminiferal tests had suffered dissolution by rain and flood waters. The assemblages were characterized by calcareous benthic species with high abundances of *Cibicides refulgens*, *Ammonia beccarii*, and *Elphidium crispum* (Table 1).

According to Akimoto and Hasegawa (1989), *Hoeglundina elegans*, which was rare in the samples, lives from 80 to 240 m depth in the outer sublittoral zone and *C. refulgens* lives from 45 to 90 m depth in the middle sublittoral zone (Fig. 2). All of the other identified species live at depths shallower than 45 m in the inner sublittoral zone, and almost half of those are epifauna, which live on rocky bottoms (Kitazato, 1981). According to Sasaki and Nojo (2005), *C. refulgens* is found on the modern coast in beach deposits; however, *H. elegans* was not found in benthic foraminiferal assemblages of the modern Hirahama coast collected in August 2003 (Fig. 2). Therefore, *H. elegans* is not carried onto the beach by annual storms or typhoons. Moreover, it is notable that many of the species observed in the tsunami deposits were found further inland than the modern beach sediments (Table 1).

Therefore, on the basis of their preferred habitats, we inferred that our foraminiferal assemblages came from the seafloor at depths shallower than 90 m. Because the most abundant species, *C. refulgens*, lives mainly at 45 m depth, the tsunami deposits were derived mainly from seafloor deposits shallower than 45 m (Fig. 2).

Table 1
Species names of calcareous benthic foraminifera from 1993 tsunami deposits at B216 and A300 (see Fig. 7) compared with modern beach sediment at Hirahama coast (Sasaki and Nojo, 2005)

Species		Sample number		Modern Hirahama coast
		B216	A300	
Ammonia beccarii (Linne)	ISZ	32	66	
Bolivina seminuda Cushman	ISZ	1		
Cibicides refulgens Montfort	MSZ	62	128	34
Cymbaloporetta bradyi (Cushman)	ISZ		4	
Discorbis subopercularis Asano	ISZ	1	10	
Elphidium cf. *advenum* (Cushman)	ISZ	2		
Elphidium crispum (Linne)	ISZ	21	16	10
Elphidium jenseni (Cushman)	ISZ	1		
Glabratella subopercularis (Asano)	ISZ			16
Guttulina sp.	ISZ	2		2
Hanzawaia nipponica Asano	ISZ	3	2	
Hoeglundina elegans (d'Orbigny)	OSZ	1	2	
Lobatula lobatula (Walter and Jacob)	ISZ	5	28	
Pararotalia nipponica (Asano)	ISZ			28
Porosorotalia makiyamae (Chiji)	ISZ	2	8	
Pseudononion japonicum Asano	ISZ	4	16	
Quinqueloculina vulgaris d'Orbigny	ISZ		2	9
Quinqueloculina sp.	ISZ	1	36	
Rosalina australis (Parr)	ISZ		4	
Rosalina bradyi (Cushman)	ISZ	4	14	1
Rosalina globularis d'Orbigny	ISZ		2	
Rosalina vilardeboana d'Orbigny	ISZ	4	10	
Rosalina sp.	ISZ		10	
Sigmoidella kagaensis Cushman and Ozawa	ISZ	1	2	1
Calcareous miscellaneous genus		3	6	
Total benthonic foraminifera counted		150	366	101

ISZ: inner sublittoral zone (shallower than 45 m); MSZ: middle sublittoral zone (between 45 m and 80–90 m depth); OSZ: outer sublittoral zone (between 80–90 m depth and 190–240 m depth); see Fig. 2.

6. Discussion

6.1. General characteristics of the 1993 tsunami deposits

In general, sand layers can be deposited in intertidal and marsh environments by channel migration, river floods, and storms, as well as by tsunami waves, so some criteria are needed to distinguish tsunami-deposited sands from sands deposited by other processes. However, few descriptions are available of the sedimentary structures and facies of onshore tsunami deposits because the tsunami run-up process is very complex and depends on the seabed and nearshore topography.

During run-up, tsunami produce various sedimentary structures, including fining-upward sequences or graded beds (Nishimura and Miyaji, 1995; Benson et al., 1997; Gelfenbaum and Jaffe, 2003), nongraded (massive) or multiple graded sheet sands (Benson et al., 1997; Gelfenbaum and Jaffe, 2003), sharp erosional bases (Nanayama et al., 2000) or flame structures at the bases of beds (Minoura and Nakata, 1994), and landward-tapering wedges of marine material (Dawson et al., 1996; Minoura et al., 1996). Gelfenbaum and Jaffe (2003) reported that some deposits contain rip-up clasts of muddy soil and, in some locations, mud caps. Current ripples and dunes in onshore tsunami deposits, formed by tsunami inflows and outflows, have been reported by Sato et al. (1995) and Nanayama et al. (2000).

The 1993 onshore tsunami deposits consist mainly of fine sand derived from the seafloor at depths shallower than 50–60 m. Consistent with findings documented in other tsunami studies, the seawards deposits are coarser, being composed of coarse sands and gravels. Furthermore, the deposits thin landwards, finally pinching out at the uppermost limit of the tsunami run-up, as was also observed by Dawson et al. (1988, 1991).

Sedimentary structures such as gravel fabrics, current ripples, and dunes in the 1993 onshore tsunami deposits, identified by the in situ peel and oriented lunchbox methods, were produced by traction currents.

Benson et al. (1997) and Gelfenbaum and Jaffe (2003) described multiple graded sand beds produced by multiple tsunami waves in British Columbia and Papua New Guinea. However, their descriptions are not supported by eyewitness accounts of the tsunami waves. In this study of the 1993 onshore tsunami deposits, we identified four sedimentary units, Unit 1, Unit 2, Unit 3, and Unit 4 in ascending order on the basis of the inferred current directions. We interpreted Units 1 and 2 as sediments deposited by the inflow and outflow events of the first run-up, and Units 3 and 4 as those deposited by the inflow and outflow events of the second run-up. This multiple-wave interpretation is confirmed by eyewitness accounts of two tsunami inundations given by the residents of Taisei.

The results of our investigation of the 1993 tsunami sediments suggest the following:

1. Units 3 and 4 were more widely distributed than Units 1 and 2 because the second run-up was larger than the first run-up. Thus, we suggest that, in general, tsunami deposits can be expected to record mainly the largest run-up during a single tsunami event.
2. Unit 4 was more widely distributed than Unit 3 because the outflow eroded the inflow deposits. Thus, we suggest that, in general, outflow can be expected to erode inflow deposits, the sediments of which are redeposited in the outflow deposits.
3. We suggest that further study of the sedimentary structures of onshore tsunami deposits would lead to better understanding of variations in flow regimes and allow flow velocities to be calculated.

6.2. Estimated hydraulic conditions during tsunami sedimentation

In this paper, we described two sedimentary facies: a gravel lobe facies and a sand-sheet facies, which must have been deposited in different sedimentary environments.

Tsunami generally strikes the coastal zone as supercritical flows. Tsutsumi et al. (2000) estimated the run-up velocity of the 1993 tsunami, from an intensity test of the constructions at Aonae on Okushiri Island, as ca. 10–18 m/s. This value is the usual flow velocity of tsunami run-up onto coasts (Shuto, 1993). In general, the flow velocity is of a tsunami controlled by coastal landforms. Although the flow velocity of the tsunami at the mouth of the Usubetsu River is unknown, a similar flow velocity to that reported by Tsutsumi et al. (2000) at Aonae (Fig. 1) on Okushiri Island can be inferred, because the Taisei site and the Aonae site have almost similar 1993 tsunami wave heights, coastal landforms, and lie at similar distances from the 1993 tsunami source area.

On this basis, we can calculate the Froude number, Fr, by Eq. (2)

$$Fr = v_1/\sqrt{gh_1} \tag{2}$$

where g is gravitational acceleration, =9.8 m/s, h_1 is water depth at the Usubetsu-bashi Bridge (tsunami height − altitude = 6.1 m − 2.0 m = 4.1 m), and flow velocity, v_1 = 10–18 m/s. Thus, Fr = 1.6–2.8. Therefore, since $Fr > 1$, the flow was supercritical between the river mouth and the Usubetsu-bashi Bridge. We infer a strongly turbulent flow between the river mouth and the Usubetsu-bashi Bridge.

The flow velocity of the run-up wave between the Usubetsu-bashi Bridge and the tsunami inundation limit is unknown. However, using Eq. (3), proposed by Matsutomi and Shuto (1995), we calculated the flow velocity from the difference in altitude (m) of the water level between the upstream site and the downstream site. Using the empirical equation based on Bernoulli's law, the flow velocity can be calculated, because all of the potential energy is converted into kinetic energy. This is an effective method of the flow velocity, v_2, over a comparatively short interval.

$$v_2 = \sqrt{2gh_2} \tag{3}$$

where h_2 is 1.3 m as the difference in altitude (m) of the water level between the upstream site (B200) and the downstream site (B460) (Fig. 4). Thus, the flow velocity, v_2 = 5.0 m/s, which represents the maximum velocity between the two sites. Therefore, we estimated the flow velocity as 0–5.0 m/s in this interval. Then, using Eq. (2), if h = 0–4.1 m and v_1 = 0–5.0 m/s, then Fr = 0–0.9. Therefore, since $Fr < 1$, the flow was subcritical between B200 and B460 (Fig. 4). Subcritical flow conditions generally indicate a traction current.

Therefore, the tsunami wave ran up the Usubetsu River in a supercritical flow. After it reached the bridge, the flow velocity rapidly decreased. Just under the bridge, a hydraulic jump occurred, which rapidly deposited the gravel lobe facies near the upstream side of the Usubetsu-bashi Bridge. After the hydraulic jump, the flow changed drastically from supercritical to subcritical. It remained subcritical and the flow velocity

gradually decreased until the tsunami inundation limit was reached. The sand-sheet facies was deposited by this traction current.

Matsutomi and Shuto (1995) estimated the outflow velocity of 1993 tsunami at the Miyano coast by a similar technique to be 2.34 m/s with a water depth of 0.28 cm. Thus, $Fr=0.2<1$. Therefore, similar subcritical flow conditions probably prevailed during the outflow along the Usubetsu River.

In summary, the gravel lobe facies of the inflows resulted from strong turbulent flow with a hydraulic jump near the bridge. But, the sand-sheet facies of both inflow and outflow deposits was produced by a traction flow under subcritical flow conditions.

6.3. Origin of the 1993 tsunami deposits

Many investigators have studied the grain-size distributions of tsunami deposits worldwide. Known tsunami deposits generally consist of medium to fine sand of marine origin with a single-mode grain-size distribution (Minoura and Nakaya, 1991; Nishimura and Miyaji, 1995; Shi et al., 1995; Dawson et al., 1996). Nevertheless, Minoura et al. (1996, 1997) reported bimodal grain distributions, determined by the settling tube method, from the 1923 Kamchatka tsunami deposits and the 1992 Flores tsunami deposits. They suggested that the coarser populations had been transported as bed load and the finer populations had been transported as suspended load. These two papers contributed significant insights into tsunami deposition processes, but they did not compare sedimentary structures between inflow and outflow deposits.

Our results showed that the grain-size distributions of the inflow and outflow deposits were clearly different. Unit 4 (outflow deposits) was composed of well-sorted fine sands with a peak at 2.5 phi (P-1 population) and a high sorting index (Fig. 10a). In contrast, Unit 3 (inflow) deposits were composed of poorly sorted medium to coarse sands with a bimodal grain-size distribution with peaks at −0.5–1.5 phi (P-2 population) and 2.5 phi (P-1 population; Fig. 10a).

Comparison of the 1993 tsunami deposits with other sand deposits in the vicinity of the study area–fluvial, coastal, and offshore sands from below 5.5 m depth (Fig. 10b)–suggests that the tsunami deposits were mainly derived from the offshore area below 5.5 m depth, where the grain size of the marine sands is 2–2.5 phi, similar to the P-1 population in the tsunami deposits. Sediments deposited during the tsunami run-up also contained coarse fluvial materials (P-2 population) (Fig. 10b).

The benthic foraminiferal assemblages also provided important information on the tsunami (Fig. 2 and Table 1). The assemblages were derived from the seafloor at depths shallower than 90 m (inner and middle sublittoral zones; Fig. 2). The dominant species showed that the main source area was depths shallower than 45 m depth. In addition, tidal shell assemblages, *Neptunea (Barbitonia) arthritica* (habitat, ca. 2 m depth), *Omphalius rusticum* (rocky coast), *Ostrea denselamellosa* (tidal area), and *P. yessoensis* (ca. 50 m depth) have been previously identified in the 1993 tsunami deposits from the Hirahama coast (Nanayama et al., 2000).

Therefore, we inferred that the P-1 population was derived mainly from offshore sediments from between 90 and 45 m depth and that these sediments were mixed with fluvial sediments (P-2 population) during the tsunami run-up (Fig. 11).

6.4. Deep-marine benthic foraminiferal tests in the tsunami deposits

In general, numerical tsunami simulations based on shallow-water theory (Shuto et al., 1990; Imamura et al., 1993) have shown that tsunami waves erode only the nearshore area and not deeper areas. Moreover, nearshore and intertidal species have previously been reported from tsunami deposits (Kon'no, 1961; Clague et al., 1999). In contrast, we found deep marine benthic foraminiferal tests, as did Okahashi et al. (2002). It was not clear, however, how benthic foraminifera from the deep seabed became incorporated in the tsunami deposits.

Therefore, we considered the threshold velocity of benthic foraminifera living between 45 and 90 m depth off Taisei. In shallow seas, the relation between tsunami propagation speed v_3 and water depth h_3 is shown by Eq. (4).

$$v_3 = \sqrt{gh_3} \tag{4}$$

where g is gravitational acceleration, $=9.8$ m/s. Furthermore, if a minute amplitude wave is assumed, then the flow velocity u of an advancing wave is expressed in terms of the water surface amplitude η as follows.

$$u = \sqrt{gh_3}\,\frac{\eta}{h_3} \tag{5}$$

If $h_3=45$–90 m and the amplitude of the tsunami wave η is assumed to be 2 m, then $u=0.93$ to 0.66 m/s.

The mean particle size of the foraminifera in our study area was 0.35–0.45 mm. Because the specific

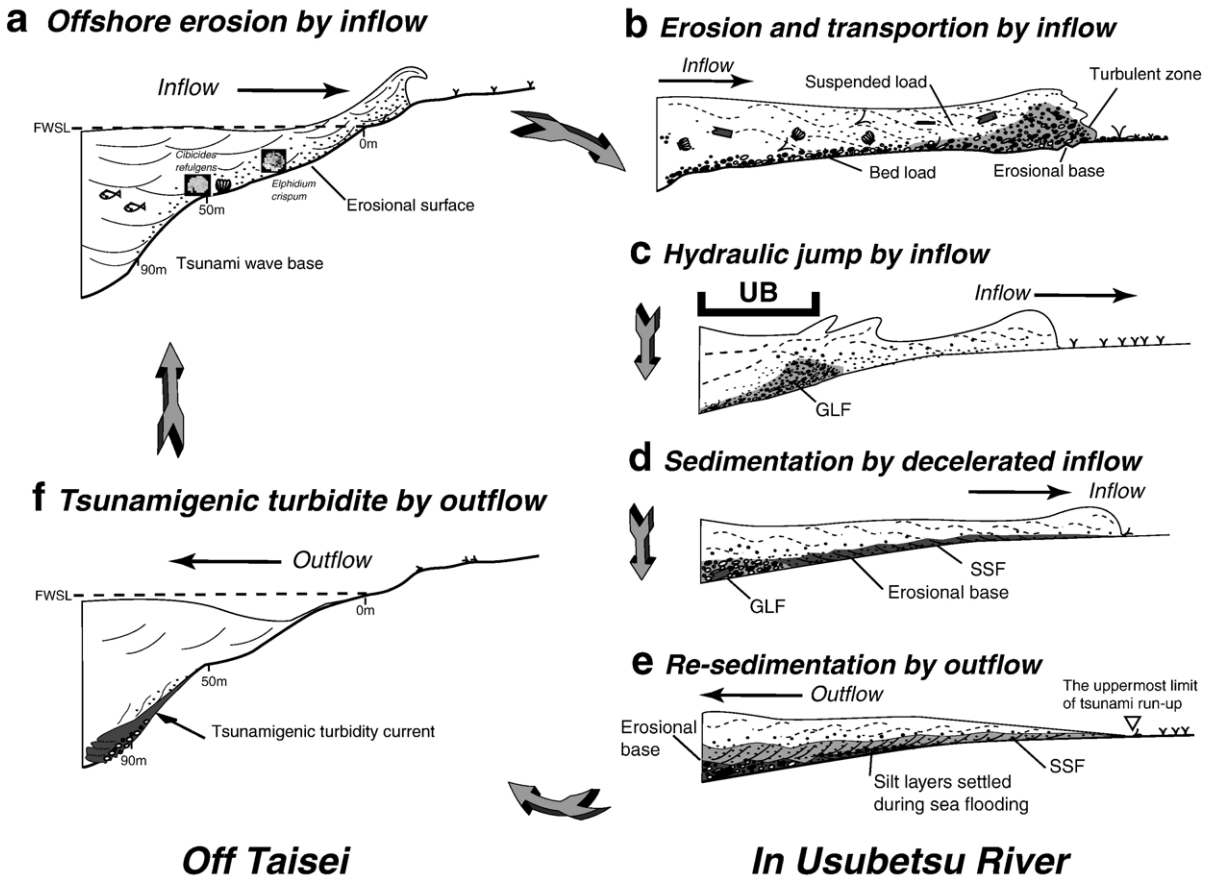

Fig. 11. Sedimentary process of the 1993 tsunami in the study area. (a) Offshore erosion by inflow, (b) erosion and transportation by inflow. (c) Hydraulic jump at the Usubetsu-bashi Bridge (UB). (d) Sedimentation by decelerated inflow prior to outflow. (e) Re-sedimentation by a turbidity current generated by the outflow. (e) Turbidity current generated by outflow. FWSL, fair weather sea level.

gravity of calcite is 2.71, or only slightly higher than that of quartz (2.65), we considered that the foraminiferal tests would behave like medium-sized sand grains. According to experimental results by Hjulstrom (1935; Hjulstrom diagram), the threshold velocity for medium-sized sand particles can be estimated as between 0.50 and 0.20 m/s. Thus, the usual flow velocity of tsunami easily exceeds this value at depths shallower than about 100 m depth.

However, we should consider the following two points. First, the threshold velocity in a tsunami, which has rapid and unpredictable flow velocity changes, would be larger than the value obtained by an experiment performed under controlled conditions such as that of Hjulstrom (1935). Second, on the actual seabed, the threshold velocity of each particle must be greater than the experimental value because under natural conditions the particles are of mixed sizes (Berg, 1986).

Therefore, benthic foraminiferal tests scattered over a comparatively deep seafloor, for example, at water depths between 45 and 90 m, can be picked up at the time of the tsunami run-up. In other words, the presence of benthic foraminiferal tests is an important criterion that can be used to identify past tsunami deposits and provides important information about the depth to which the sea was agitated by the tsunami waves.

6.5. Tsunami sedimentation after the 1993 earthquake

From our results, we reconstructed the sedimentary processes responsible for the 1993 tsunami deposits in the mouth of the Usubetsu River as follows (Fig. 11):

(a) The 1993 tsunami originated at the earthquake epicenter northwest of Okushiri Island, and then propagated and struck and eroded the coastal shelf slope off Taisei. The eroded marine sands were

then transported onto the land by the turbulent flow of the tsunami waves (Fig. 11a).

(b) From a hydrologic perspective, the flow became highly turbulent during the tsunami run-up under supercritical flow conditions in the lower course of the Usubetsu River. Flow velocity and energy decreased during the run-up process, but fluvial coarse sands and gravels were eroded from the riverbed and transported farther inland (Fig. 11b).

(c) As the hydrodynamic energy of the tsunami decreased at the Usubetsu-bashi Bridge, a hydraulic jump occurred, resulting in the rapid deposition of a gravel lobe facies near the bridge (Fig. 11c).

(d) Beyond that point, extensive sand sheets carried by traction currents were deposited to the run-up limit of the tsunami under subcritical flow conditions (Fig. 11d).

(e) After the run-up limit was reached, a thin silt layer containing many plant fragments settled during the flooding. When the influx of water flowed back into the ocean, the outflow rearranged the onshore sediments deposited during run-up, creating sedimentary structures formed by traction currents under subcritical flow conditions (Fig. 11e).

(f) As the outflow moved down the submarine slope of the shelf off Taisei, it may have generated a turbidity current that deposited a tsunamigenic turbidite (Fig. 11f).

7. Conclusions

1. We recognized only two lithofacies, a gravel lobe facies (GLF) and a sand-sheet facies (SSF), in the 1993 tsunami deposits. The gravel lobe facies was rapidly deposited by a hydraulic jump. On the other hand, the sand-sheet facies with current ripples and dunes was deposited by a traction current under subcritical flow conditions.
2. We identified four stratigraphic units: Units 1 through 4, in ascending order. We interpreted Units 1 and 2 as deposits from the inflow and outflow events of the first run-up, and Units 3 and 4 as deposits from the inflow and outflow events of the second run-up.
3. Units 3 and 4 were more widely distributed and coarser grained than Units 1 and 2 because the second run-up was larger than the first run-up. Furthermore, Unit 4 was more widely distributed than Unit 3 because the outflow eroded the inflow deposits.
4. Grain-size distributions of the inflow and outflow deposits were clearly different. Unit 4 deposits had a peak at 2.5 phi (P-1 population). In contrast, Unit 3 deposits had a bimodal distribution with peaks at −0.5–1.5 phi (P-2 population) and at 2.5 phi (P-1 population). A comparison of the tsunami deposits with other sedimentary deposits near the study area showed that the tsunami deposits were mainly derived from depths below 5.5 m depth in the offshore area, where marine sands were about 2–2.5 phi in size, and from coarse (0.5–2 phi) fluvial materials eroded during the tsunami run-up.
5. According to our calculations, benthic foraminiferal tests from the comparatively deep seabed (up to 100 m depth) can be picked up during tsunami run-up and included in tsunami deposits.

Acknowledgments

We thank Dr. Brian F. Atwater (US Geological Survey), Drs. K. Satake and K. Shimokawa (Active Fault Research Center, Geological Survey of Japan/AIST), who provided valuable comments. Thanks are also due to Dr. Keith A. W. Crook and two reviewers for their valuable suggestions for the improvement of the paper. Dr. T. Sagayama (Geological Survey of Hokkaido) collected sand samples from off Taisei town. The town office of Taisei provided photographs and survey data. This research has been supported in part by Grant-in-aid for Scientific Research from the Ministry of Education, Science and Culture of Japan (No. 16540423) and Grant for Environmental Research Projects by the Sumitomo Foundation (No. 033209).

References

Akimoto, K., Hasegawa, S., 1989. Bathymetric distribution of the recent benthic foraminifers around Japan as a contribution to the new paleobathymetric scale. Memoirs of the Geological Society of Japan 32, 229–240 (in Japanese, with English abstract).

Atwater, B.F., 1987. Evidence for great Holocene earthquakes along the outer coast of Washington state. Science 236, 942–944.

Atwater, B.F., 1992. Geologic evidence for earthquakes during the past 2000 years along the Copalis River, southern coastal Washington. Journal of Geophysical Research 97, 1901–1919.

Atwater, B.F., Moore, A.L., 1992. A tsunami about 1000 years ago in Puget Sound, Washington. Science 258, 1614–1617.

Benson, B.E., Grimm, K.A., Clague, J.J., 1997. Tsunami deposits beneath tidal marshes on northwestern Vancouver Island, British Columbia. Quaternary Research 48, 192–204.

Berg, R.R., 1986. Reservoir Sandstone. Prentice Hall, Englewood Cliffs, New Jersey. 481 pp.

Bondevik, S., Sevendsen, J.I., Mangerud, J., 1997. Tsunami sedimentary facies deposited by the Stregga tsunami in shallow

marine basins and coastal lakes, western Norway. Sedimentology 44, 1115–1131.

Clague, J.J., Bobrowsky, P.T., 1994. Tsunami deposits beneath tidal marshes on Vancouver Island, British Colombia. Geological Society of America Bulletin 106, 1293–1303.

Clague, J.J., Hutchinson, I., Mathewes, R.W., Patterson, R.T., 1999. Evidence for late Holocene tsunamis at Catala Lake, British Columbia. Journal of Coastal Research 15, 45–60.

Dawson, A.G., Long, D., Smith, D.E., 1988. The Storegga slides: evidence from Eastern Scotland for a possible tsunami. Marine Geology 82, 271–276.

Dawson, A.G., Foster, I.D.L., Shi, S., Smith, D.E., Long, D., 1991. The identification of tsunami deposits in coastal sediment sequences. Science of Tsunami Hazards 9, 73–82.

Dawson, A.G., Shi, S., Dawson, S., Takahashi, T., Shuto, N., 1996. Coastal sedimentation associated with the June 2nd and 3rd, 1994 Tsunami in Rajegwesi, Java. Quaternary Science Reviews 15, 901–912.

Ganzawa, Y., Kito, N., Sadakata, N., 1995. Tsunami of the 1993 southwest off Hokkaido earthquake and refuge behavior of people: in the case of the Taisei town in Hokkaido, Japan. Earth Science (Chikyu Kagaku) 49, 379–390 (in Japanese, with English abstract).

Gelfenbaum, G., Jaffe, B., 2003. Erosion and sedimentation from the 17 July 1998 Papua New Guinea tsunami. Pure and Applied Geophysics 160, 1969–1999.

Hjulstrom, F., 1935. Studies of morphological activity of rivers as illustrated by the River Fyris. Bulletin of Geological Institute, University of Uppsala 25, 221–527.

Hutchinson, I., Clague, J.J., Mathewes, R.W., 1997. Reconstructing the tsunami record on an emerging coast: a case study of Kanim Lake, Vancouver Island, British Columbia, Canada. Journal of Coastal Research 13, 545–553.

Imamura, F., Shuto, N., Ide, S., Yoshida, Y., Abe, K., 1993. Estimate of the tsunami source of the 1992 Nicaraguan earthquake from tsunami data. Geophysical Research Letters 20, 1515–1518.

Kitazato, H., 1981. Observation of behavior and mode of life of benthic foraminifers in the laboratory. Geoscience Reports of Shizuoka University 6, 61–71 (in Japanese, with English abstract).

Kon'no, E., 1961. Geological observations of the Sanriku coastal region damaged by the tsunami due to the Chile earthquake in 1960. Contributions from the Institute of Geology and Paleontology, Tohoku University 52 (40 pp.).

Kumon, F., Tateishi, M., 1998. How to Study Clastic Sediments? 2nd ed. Geoscience Series No. 29. The Association for Geological Collaboration in Japan (AGCJ), Tokyo. 399 pp. (in Japanese).

Matsutomi, H., Shuto, N., 1995. Tsunami inundation depth, current velocity and degree of damage to houses. Proc. of the Intl. Workshop on Wind and Earthquake Eng. for Offshore and Coastal Facilities, pp. 195–199.

Minoura, K., Nakata, T., 1994. Discovery of an ancient tsunami deposit in coastal sequences of southwest Japan: verification of a large historic tsunami. Island Arc 3, 66–72.

Minoura, K., Nakaya, S., 1991. Traces of tsunami preserved in intertidal lacustrine and marsh deposits: some examples from northeast Japan. Journal of Geology 99, 265–287.

Minoura, K., Nakaya, S., Uchida, M., 1994. Tsunami deposits in a lacustrine sequence of the Sanriku coast, northeast Japan. Sedimentary Geology 89, 25–31.

Minoura, K., Gusiakov, V.G., Kurbatov, A., Takeuchi, S., Svendsen, J.I., Bondevik, S., Oda, T., 1996. Tsunami sedimentation associated with the 1923 Kamchatka earthquake. Sedimentary Geology 106, 145–154.

Minoura, K., Imamura, F., Takahashi, T., Shuto, N., 1997. Sequence of sedimentation processes caused by the 1992 Flores tsunami: evidence from Babi Island. Geology 28, 59–62.

Minoura, K., Imamura, F., Kuran, U., Nakamura, T., Papadopoulas, G.A., Takahashi, T., Yalciner, A.C., 2000. Discovery of Minoan tsunami deposits. Geology 28, 59–62.

Moore, A.L., 2000. Landward fining in onshore gravel as evidence for a late Pleistocene tsunami on Molokai, Hawaii. Geology 28, 247–250.

Moore, J.G., Moore, G.W., 1984. Deposit from a giant wave on the island of Lanai, Hawaii. Science 226, 1312–1315.

Nanayama, F., Shigeno, K., 1998. How to make oriented samples of loose sediments by lunch box and easy-dry bond. Chishitsu News 523, 52–56 (in Japanese).

Nanayama, F., Sigeno, K., Satake, K., Shimokawa, K., Koitabashi, S., Miyasaka, S., Ishii, M., 2000. Sedimentary differences between the 1993 Hokkaido–Nansei-oki tsunami and the 1959 Miyakojima typhoon at Taisei, southwestern Hokkaido, northern Japan. Sedimentary Geology 135, 255–264.

Nanayama, F., Satake, K., Furukawa, R., Shimokawa, K., Atwater, B.F., Shigeno, K., Yamaki, S., 2003. Unusually large earthquakes inferred from tsunami deposits along the Kuril trench. Nature 424, 660–663.

Nishimura, Y., Miyaji, N., 1995. Tsunami deposits from the 1993 southwest Hokkaido earthquake and the 1640 Hokkaido Komagatake eruption, northern Japan. Pure and Applied Geophysics 144, 720–733.

Okahashi, H., Akimoto, K., Mitamura, M., Hirose, K., Yasuhara, M., Yoshikawa, S., 2002. Event deposits found in marsh sediments at Osatsu, Toba City, Mie Prefecture: identification of tsunami deposits using benthic foraminiferal fossils. Chikyuu 24, 698–703 (in Japanese).

Pinegina, T.K., Bourgeois, J., 2001. Historical and paleo-tsunami deposits on Kamchatka, Russia: long-term chronologies and long-distance correlations. Natural Hazards and Earth System Sciences 1, 177–185.

Sagayama, T., Uchida, Y., Osawa, M., Suga, K., Hamada, S., Murayama, Y., Nishina, K., 2000. Environment of submarine geology in the coastal area of Hokkaido. 2. Southwest Hokkaido. Special Report of Geological Survey of Hokkaido, vol. 29. 74 pp. (in Japanese, with English abstract).

Sasaki, N., Nojo, A., 2005. Coastal sands and foraminiferal species in Hokkaido. http://env.iwa.hokkyodai.ac.jp/%7Enojo/ind2/naochin/index.html (in Japanese).

Sato, H., Shimamoto, A., Kawamoto, E., 1995. Onshore tsunami deposits caused by 1993 southwest Hokkaido and 1983 Japan Sea earthquakes. Pure and Applied Geophysics 144, 693–717.

Shi, S., Dawson, A.G., Smith, D.E., 1995. Coastal sedimentation associated with December 12th, 1992 tsunami in Flores, Indonesia. Pure and Applied Geophysics 144, 525–536.

Shigeno, K., Nanayama, F., Satake, K., Shimokawa, K., 2000. Correlation between tsunami deposits and inundation area for the 1993 Hokkaido–Nansei-oki earthquake tsunami in Taisei Town, western side of Oshima peninsula, southwest Hokkaido. Geological Survey of Japan Interim Report, No. EQ/00/2, pp. 19–41 (in Japanese, with English abstract).

Shimamoto, T., Tsutsumi, A., Kawamoto, E., Miyawaki, M., Sato, H., 1995. Field survey report on tsunami disasters caused by the 1993 Southwest Hokkaido Earthquake. Pure and Applied Geophysics 144, 665–691.

Shuto, N., 1993. Tsunami intensity and disasters. Tsunami in the World, pp. 197–216.

Shuto, N., Goto, C., Imamura, F., 1990. Numerical simulation as a means of warning for near-field tsunami. Coastal Engineering of Japan 33, 173–193 (in Japanese).

Tsuji, Y., Kato, K., Satake, A., 1994. Heights and damage of the tsunami of the 1993 Hokkaido–Nansei-oki earthquake in residential areas on the coast of the Hokkaido mainland. Bulletin of Earthquake Research Institute, University of Tokyo 69, 67–106 (in Japanese, with English abstract).

Tsutsumi, A., Shimamoto, T., Kawamoto, E., Logan, J.M., 2000. Near-shore flow velocity of Southwest-Hokkaido-Earthquake Tsunami. Journal of Waterway, Port, and Coastal, and Ocean Engineering, ASCE, vol. 126, pp. 136–143.

Wright, C., Mella, A., 1963. Modifications to the soil pattern of south–central Chile resulting from seismic and associated phenomena during the period May to August 1960. Bulletin of the Seismological Society of America 53, 1367–1402.